

# CrystEngComm

Accepted Manuscript



This is an *Accepted Manuscript*, which has been through the Royal Society of Chemistry peer review process and has been accepted for publication.

*Accepted Manuscripts* are published online shortly after acceptance, before technical editing, formatting and proof reading. Using this free service, authors can make their results available to the community, in citable form, before we publish the edited article. We will replace this *Accepted Manuscript* with the edited and formatted *Advance Article* as soon as it is available.

You can find more information about *Accepted Manuscripts* in the [Information for Authors](#).

Please note that technical editing may introduce minor changes to the text and/or graphics, which may alter content. The journal's standard [Terms & Conditions](#) and the [Ethical guidelines](#) still apply. In no event shall the Royal Society of Chemistry be held responsible for any errors or omissions in this *Accepted Manuscript* or any consequences arising from the use of any information it contains.

## Template-free synthesis of $\beta$ - $\text{Na}_{0.33}\text{V}_2\text{O}_5$ microspheres as cathode materials for lithium-ion batteries

*Qinguang Tan,<sup>a,+</sup> Qinyu Zhu,<sup>a,+</sup> Anqiang Pan,<sup>a,\*</sup> Yaping Wang<sup>a</sup>, Yan Tang,<sup>a</sup> Xiaoping Tan<sup>a</sup>, Shuquan Liang,<sup>a,\*</sup> and Guozhong Cao<sup>b,\*</sup>*

<sup>a</sup> School of Materials Science & Engineering, Central South University, Changsha, Hunan, 410083, China

<sup>b</sup> Department of Materials Science & Engineering, University of Washington, Seattle, 98195, USA

<sup>+</sup> The authors are contributed equally to this manuscript.

\* Corresponding authors: [pananqiang@csu.edu.cn](mailto:pananqiang@csu.edu.cn) (A.Q. Pan); [lsq@mail.csu.edu.cn](mailto:lsq@mail.csu.edu.cn) (S.Q. Liang); [gzcao@u.washington.edu](mailto:gzcao@u.washington.edu) (G.Z. Cao)

### Abstract

In this work, hierarchical three-dimensional (3D)  $\beta$ - $\text{Na}_{0.33}\text{V}_2\text{O}_5$  microspheres have been synthesized for the first time by a simple solvothermal reaction with subsequent annealing treatment. The hierarchical microspheres are self-assembled from nanosheet subunits during the solvothermal process. Simultaneously, various hierarchical microspheres with different subunits can be produced by altering the solvothermal solution. After annealing in air, the solvothermal product can be converted into  $\beta$ - $\text{Na}_{0.33}\text{V}_2\text{O}_5$  with well retained structure. As cathode material for lithium ion batteries, the as-prepared 3D microspheres exhibit high capacity and good rate capability. The superior electrochemical performance is attributed to the three-dimensional unique hierarchical microstructures, which mimic the advantageous of nano- and micro-structures.

**Keywords:** sodium vanadium oxide, solvothermal reaction, three-dimensional microstructures, lithium-ion batteries

## 1. Introduction

Recently, three-dimensional (3D) nanostructured materials have attracted considerable attention due to their superior physical and chemical properties.<sup>1-5</sup> In particular, they are broadly studied as electrodes for Lithium ion batteries (LIBs) because of the capability to keep the structural integrity, high packing density and good lithium storage properties.<sup>6-9</sup> Moreover, the characteristic hierarchical structures are believed to have better abilities to suppress the agglomeration, facilitate the electrolyte penetration and accommodate the volume change upon cycling.<sup>10-12</sup> And the nanosized building blocks also could effectively reduce the lithium diffusion distance, which could significantly improve the rate capability and capacity retention.<sup>10, 13, 14</sup> To date, the hierarchical micro/nanostructures, such as porous frameworks<sup>1, 15-18</sup>, hollow structured microspheres<sup>13, 19</sup> urchin-like microflowers<sup>20, 21</sup> have been fabricated to investigate their electrochemical properties. However, the majority of the reports are based on metal oxides with simple composition. It is still a big challenge to fabricate hierarchical lithium/sodium transition metal oxides with complex compositions, such as  $\text{LiMn}_2\text{O}_4$  and  $\text{Na}_{0.33}\text{V}_2\text{O}_5$ , which significantly limits their applications.<sup>22-29</sup>

Vanadium oxides and their derivatives have attracted research interests as alternative cathode materials for LIBs for decades, mainly because of their high specific capacities, low cost and abundant resources.<sup>16, 29-37</sup> Among the vanadium oxide derivatives, the  $\beta$ -phase  $\text{Na}_{0.33}\text{V}_2\text{O}_5$  is believed to be a promising candidate due to its 3D tunneled crystal structure and high capacity.<sup>38-41</sup> To date, low dimensional  $\beta$ - $\text{Na}_{0.33}\text{V}_2\text{O}_5$  nanowires<sup>42,43</sup> and mesoporous nanoflakes<sup>39</sup> have been reported to improve their electrochemical performance. However, the synthesis of  $\beta$ - $\text{Na}_{0.33}\text{V}_2\text{O}_5$  hierarchical structures is rarely reported.

Herein, we reported the fabricating of  $\beta$ - $\text{Na}_{0.33}\text{V}_2\text{O}_5$  hierarchical microspheres by a solvothermal

approach with following process in air. The solvothermally prepared microspheres are assembled from small nanosheets and the structures can be safely retained after calcinations in air. As cathode materials for lithium ion batteries, the  $\beta$ - $\text{Na}_{0.33}\text{V}_2\text{O}_5$  microspheres exhibit high capacity and good rate capability.

## 2. Experimental Section

*Materials preparation:*  $\text{V}_2\text{O}_5$  (0.36g) and  $\text{H}_2\text{C}_2\text{O}_4 \cdot 2\text{H}_2\text{O}$  in a molar ratio of 1:3 were dissolved in 12 mL of distilled water under vigorous stirring at 60 °C for several hours until a clear blue solution was formed. Then,  $\text{NaHCO}_3$  with different molar ratio of (Na:V= 1:4, 1:6 and 1:3) were separately added into the above-prepared solution under stirring for 20 minutes. After that, 60 mL of isobutanol was added to make the mixture solution, which was transferred into a sealed 100 mL Teflon container and treated in an electrical oven at 180 °C for 48 h. The obtained precursors were collected by centrifugation and washed with pure ethanol for two times, followed by drying at 70 °C overnight. The as-prepared precursors were annealed in air at 400 °C for 3 h with a heating rate of 1 °C  $\text{min}^{-1}$ . The as-synthesized products obtained from the molar ratio of Na:V = 1:4, 1:6 and 1:3 were designated as NVO-1, NVO-2 and NVO-3, respectively.

*Materials Characterization:* TG and DSC analysis were performed on a combined Differential Scanning Calorimetry Thermogravimetric Analysis instrument (Netzsch STA449C, Germany). Crystallographic phases of all the products were investigated by powder X-ray diffraction (XRD, Rigaku D/max2500) with  $\text{Cu K}\alpha$  ( $\lambda=1.5406 \text{ \AA}$ ) radiation. Morphologies of samples were examined by field-emission scanning electron microscopy (SEM, FEI Nova NanoSEM 230) and transmission electron microscopy (TEM; JEOL-JEM-2100F transmission electron microscope).

*Electrochemical Measurements:* The working cathode slurry was prepared by dispersing the

$\beta$ - $\text{Na}_{0.33}\text{V}_2\text{O}_5$ , acetylene black and poly-(vinylidene fluoride) (PVDF) binder in an N-methylpyrrolidone solution at a weight ratio of 70:20:10. The slurry was painted on aluminum foil and dried in a vacuum oven at 110 °C overnight prior to coin-cell assembly. Lithium foil was used as the current collector and reference electrode, and 1.0M  $\text{LiPF}_6$  in ethyl carbonate/dimethyl carbonate (1:1v/v ratio) was used as the electrolyte. Cyclic voltammetry (CV) measurements were performed on an electrochemical workstation (CHI604E, China). The galvanostatic charge/discharge performances of the electrodes were evaluated at room temperature using a Land Battery Tester (Land CT 2001A, China). The electrochemical impedance spectrometry (EIS) was carried out on a ZAHNER-IM6ex electrochemical workstation in the frequency range of 100 KHz to 10 mHz.

### 3. Results and discussion

Figure 1 shows the SEM images of the solvothermally prepared microspheres precursor at different magnifications. As shown in Figure 1a and 1b, the solvothermal products from the molar ratio of Na:V=1:4 are of spherical morphology and the diameter of which is about 4 $\mu\text{m}$ . The microspheres are monodispersed. The higher magnification SEM image (Fig. 1c) further reveals the detailed structures of microspheres, which are assembled from discrete nanosheets with a thickness of about 30 nm. The formation of hierarchical microspheres in the solvothermal process is attributed to the mixed solvents of isobutanol and water. The whole solvent can be considered as the gathering of small water and isobutanol droplets, and the precursor subunits are formed within the droplets. When the subunits grow big enough, they will break the limitation of the volume limitation of small droplets and the subunits will merge together in order to reduce the surface energy to reach a more thermodynamical stable state. Therefore, the hierarchical microspheres will be formed. As shown in Fig. 2a and b, when  $\text{NaHCO}_3$  with a molar ratio of Na:V=1:6 was added into the solvothermal

solution, nanosheet structured microflowers are obtained after solvothermal treatment. The diameter of the microflowers was much smaller, ranging from 2 to 3  $\mu\text{m}$ . As shown in Figure 2c and d, urchin-like NVO-3 nano-/microstructures could be produced when  $\text{NaHCO}_3$  with a higher molar ratio of  $\text{Na}:\text{V}=1:3$ . The urchin-like subunits were composed of nanobelts with a length about 3  $\mu\text{m}$ . And the urchin-like microspheres were the largest among the three solvothermally prepared samples. When more  $\text{NaHCO}_3$  was added, the subunits of the hierarchical microstructures changed from nanosheets to nanobelts. The morphology change may be raised from the higher concentration of  $\text{Na}^+$  ions, which may serve as the nuclei centers for the precursors. When more  $\text{Na}^+$  ions are provided in the solvothermal solution, more subunits start to grow and the species in the solution are depleted much faster, so that the smaller subunits (nanobelts) are formed. This behavior is a little similar to the previous report on the synthesis of  $\text{VO}_2$  microstructures.<sup>20</sup> The results demonstrated that the hierarchical microstructures with different morphologies can be obtained by simply altering the addition amount of the  $\text{NaHCO}_3$ .

Figure 3 shows the TG and DSC results of the precursor microspheres calcined in air using a heating rate of  $10\text{ }^\circ\text{C min}^{-1}$ . The first weight-loss below  $250\text{ }^\circ\text{C}$  is attributed to the evaporation of the physically absorbed and crystalline hydrate in the precursor. The main weight loss on TG curve and the corresponding exothermic peak in the DSC curve at  $366\text{ }^\circ\text{C}$  are ascribed to the formation of  $\beta\text{-Na}_{0.33}\text{V}_2\text{O}_5$ . The sharp endothermic peak on the DSC curve at  $582\text{ }^\circ\text{C}$  suggests the melting of  $\beta\text{-Na}_{0.33}\text{V}_2\text{O}_5$ . After annealing in air, the precursor microspheres can be converted to  $\beta\text{-Na}_{0.33}\text{V}_2\text{O}_5$  with well preserved morphologies. Fig. 4a shows the XRD pattern of the calcination product (NVO-1) in air at a relatively low temperature of  $400\text{ }^\circ\text{C}$  for 3h, which can be indexed into a  $\beta\text{-Na}_{0.33}\text{V}_2\text{O}_5$  phase (space group:  $A2/m(12)$ , JCPDS card 86-0120).<sup>38, 39</sup> A panoramic view of the product (Fig. 4b)

demonstrates that the morphologies of the microspheres are well preserved from the solvothermal products after annealing in air. The space between neighboring nanosheets is clearly detected (Fig. 4c). The nanosheet subunits shrunk to smaller nanosheets during the annealing process, which may be attributed to the recrystallization of the precursor when it is converted into  $\beta\text{-Na}_{0.33}\text{V}_2\text{O}_5$ . The TEM image (see Fig. 4d) reveals the microspheres are composed of nanosheet subunits and the existence of path way from outside to inside. The good porosity is beneficial for the electrolyte penetration into the electrode materials. The hierarchical nature of  $\beta\text{-Na}_{0.33}\text{V}_2\text{O}_5$  microspheres is further evaluated by the nitrogen adsorption-desorption measurement and the results are shown in Fig. 5. The isothermal curve exhibit a typical  $\text{IV}$  type, indicating a macroporous characteristic. The measured Brunauer-Emmett-Teller (BET) area for  $\beta\text{-Na}_{0.33}\text{V}_2\text{O}_5$  microspheres is  $12.5 \text{ m}^2 \text{ g}^{-1}$ . Barrett-Joyner-Halenda (BJH) calculations disclose that the pore size distribution is in the range of 3-20 nm, which has a good correspondence with the TEM image.

The  $\beta\text{-Na}_{0.33}\text{V}_2\text{O}_5$  microspheres were assembled into coin-cells and evaluated as a cathode material for LIBs. Fig. 6a shows the typical cyclic voltammetry(CV) curve of the  $\beta\text{-Na}_{0.33}\text{V}_2\text{O}_5$  microspheres at a scan rate of  $0.1 \text{ mV s}^{-1}$  between 1.5 and 4.0 V vs.  $\text{Li/Li}^+$ . During the cathodic scan, five cathodic peaks located at 3.22, 2.88, 2.46, 2.20 and 1.88 V are observed, indicating the multiple-step lithium ions intercalation process.<sup>35-37</sup> Fig. 6b shows both the representative discharge-charge profiles of the  $\beta\text{-Na}_{0.33}\text{V}_2\text{O}_5$  electrode between 1.5 and 4.0 V at the current densities of 50, 600 and 1000  $\text{mA g}^{-1}$ . The potentials for the five plateaus on the discharge profiles of the first cycle are consistent well with the CV results. The  $\beta\text{-Na}_{0.33}\text{V}_2\text{O}_5$  microspheres deliver high initial specific capacities of 249, 216, 157  $\text{mA h g}^{-1}$  at current densities of 50, 600 and 1000  $\text{mA g}^{-1}$ , respectively, indicating the good rate capability of the electrode material. Fig. 6c shows the cycling

performance of the  $\beta\text{-Na}_{0.33}\text{V}_2\text{O}_5$  microspheres at a current density of  $1000 \text{ mA g}^{-1}$ . It delivers an initial discharge capacity of  $157 \text{ mA h g}^{-1}$  and retains a specific discharge capacity of  $111 \text{ mA g}^{-1}$  after 35 cycles. The average capacity fading rate per cycle is 0.8%. The good cycling performance at high current density can be attributed to the novel three dimensional microstructures assembled from nanosheets building blocks. The hierarchical 3D microspheres can limit the self-aggregation upon cycling. The large space between neighboring subunits can provide easy path ways for electrolyte penetration and the nanosized subunits can shorten lithium ion diffusion and the electron transportation distances, thus allowing the electrode to obtain good rate capability and cyclic stability. In order to study the transport kinetics of the electrochemical properties of the microspheres, the typical electrochemical impedance spectra of the electrodes were performed and the Nyquist plots are shown in Fig. 6d. The impedance spectra consist of a depressed semicircle in the high frequency region and straight line in the low-frequency region. The semicircle is assign to the formation of solid electrolyte interface (SEI) film and contact resistance, and the straight line is associated with the diffusion of  $\text{Li}^+$  in the electrode materials. In the equivalent circuit model inset Fig. 6d,  $R_1$  consist of the electrolyte resistance and ohmic resistances of cell components.  $R_2$  is the resistance of SEI films while  $R_3$  is the charge transfer resistance of electrochemical reaction. The value of  $R_3$  increase with cycling due to the increasing thickness of SEI film and the irreversible phase transformation, which is commonly seen as a dominant effect for the capacity fading of vanadium based cathodes.<sup>44</sup>

<sup>45</sup> As shown in Nyquist plots, for the fresh electrode, the charge transfer resistance value is  $121.6\Omega$ . When the electrode was evaluated for 35 cycles, the charge transfer resistance increases to  $181.3\Omega$ , indicating a slight increase of charge transfer resistance but a lower increasing rate comparing with that of the mesoporous  $\beta\text{-Na}_{0.33}\text{V}_2\text{O}_5$  electrode.<sup>39</sup> The small charge-transfer resistance can be

attributed to the unique hierarchical structures, which shorten the diffusion pathways and improve the structure stability during the cycling processes. To further investigate the structure stability of  $\beta\text{-Na}_{0.33}\text{V}_2\text{O}_5$  electrodes, the morphology of the  $\beta\text{-Na}_{0.33}\text{V}_2\text{O}_5$  microspheres after cycling process was characterized by SEM. As shown in Fig. 7, after cycling at  $1000\text{ mA g}^{-1}$  for 35 cycles, it is interesting to find that the hierarchical structures of the microspheres can be retained, which indicate the good structural stability of the hierarchical structures..

### Conclusions

In summary, 3D hierarchical  $\beta\text{-Na}_{0.33}\text{V}_2\text{O}_5$  microspheres have been successfully synthesized through a simple solvothermal method with following annealing process. The morphologies of the solvothermally prepared microstructures can be adjusted by changing the addition amount of  $\text{NaHCO}_3$ . The nanosheet-assembled microspheres can be converted into  $\beta\text{-Na}_{0.33}\text{V}_2\text{O}_5$  with good structural reservation after annealing. As cathode material for LIBs, the  $\beta\text{-Na}_{0.33}\text{V}_2\text{O}_5$  microspheres exhibit high rate capability and enhanced cycling stability.

### Acknowledgment

This work was supported by National High-tech R&D Program (863, Grant No. 2013AA110106), the National Natural Science Foundation of China (No. 51374255, 51202323), Program for New Century Excellent Talents in University (NCET-13-0594), Research Fund for the Doctoral Program of Higher Education of China (No. 201301621200), Natural Science Foundation of Hunan Province, China (14JJ3018), Lie-Ying and Sheng-Hua Program of Central South University.

### References

1. Q. An, F. Lv, Q. Liu, C. Han, K. Zhao, J. Sheng, Q. Wei, M. Yan and L. Mai, *Nano Lett.*, 2014, 14, 6250-6256.

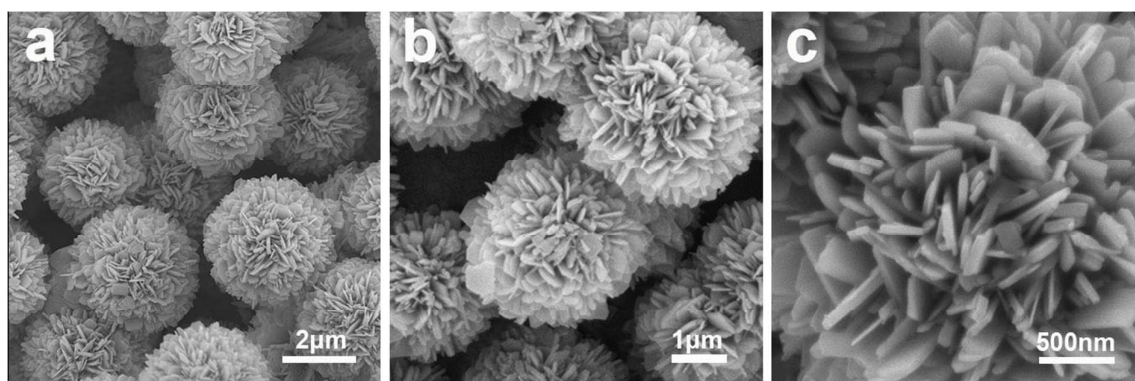
2. J. Bai, X. Li, G. Liu, Y. Qian and S. Xiong, *Adv. Funct. Mater.*, 2014, 24, 3012-3020.
3. J. S. Chen, D. Luan, C. M. Li, F. Y. Boey, S. Qiao and X. W. Lou, *Chem. Commun.*, 2010, 46, 8252-8254.
4. X. Fan, J. Shao, X. Xiao, L. Chen, X. Wang, S. Li and H. Ge, *J. Mater. Chem. A*, 2014, 2, 14641.
5. C. Cheng, W. Ren and H. Zhang, *Nano Energy*, 2014, 5, 132-138.
6. Z. Fang, Q. Wang, X. Wang, F. Fan, C. Wang and X. Zhang, *Mater. Res. Bull.*, 2013, 48, 4935-4941.
7. X. Lai, J. E. Halpert and D. Wang, *Energy Environ. Sci.*, 2012, 5, 5604.
8. D. Li, Q. Qin, X. Duan, J. Yang, W. Guo and W. Zheng, *ACS Appl. Mater. Interfaces*, 2013, 5, 9095-9100.
9. L. Hu, H. Zhong, X. Zheng, Y. Huang, P. Zhang and Q. Chen, *Sci. Rep.*, 2012, 2, 986.
10. L. Liu, Q. Fan, C. Sun, X. Gu, H. Li, F. Gao, Y. Chen and L. Dong, *J. Power Sources*, 2013, 221, 141-148.
11. X. W. Lou, C. Yuan and L. A. Archer, *Adv. Mater.*, 2007, 19, 3328-3332.
12. X. W. Lou and L. A. Archer, *Adv. Mater.*, 2008, 20, 1853-1858.
13. A. Pan, H. B. Wu, L. Yu and X. W. Lou, *Angew. Chem. Int. Ed.*, 2013, 52, 2226-2230.
14. C. Nethravathi, C. R. Rajamathi, M. Rajamathi, U. K. Gautam, X. Wang, D. Golberg and Y. Bando, *ACS Appl. Mater. interfaces*, 2013, 5, 2708-2714.
15. R. B. Rakhi, W. Chen, M. N. Hedhili, D. Cha and H. N. Alshareef, *ACS Appl. Mater. Interfaces*, 2014, 6, 4196-4206.
16. C. Zhang, Z. Chen, Z. Guo and X. W. Lou, *Energy Environ. Sci.*, 2013, 6, 974.

17. L. Huang, X. Zhao, L. Zhang, L. Y. Shi, J. P. Zhang and D. S. Zhang, *Nanoscale*, 2015, 7, 2743-2749.
18. S. Cai, D. Zhang, L. Shi, J. Xu, L. Zhang, L. Huang, H. Li and J. Zhang, *Nanoscale*, 2014, 6, 7346-7353.
19. J. Zhu, Z. Yin, D. Yang, T. Sun, H. Yu, H. E. Hoster, H. H. Hng, H. Zhang and Q. Yan, *Energy Environ. Sci.*, 2013, 6, 987.
20. C. Niu, J. Meng, C. Han, K. Zhao, M. Yan and L. Mai, *Nano Lett.*, 2014, 14, 2873-2878.
21. H. Li, D. Zhang, P. Maitarad, L. Shi, R. Gao, J. Zhang and W. Cao, *Chem. Commun.*, 2012, 48, 10645-10647.
22. K. Kim do, P. Muralidharan, H. W. Lee, R. Ruffo, Y. Yang, C. K. Chan, H. Peng, R. A. Huggins and Y. Cui, *Nano Lett.*, 2008, 8, 3948-3952.
23. S. Liang, T. Chen, A. Pan, D. Liu, Q. Zhu and G. Cao, *ACS Appl. Mater. Interfaces*, 2013, 5, 11913-11917.
24. Y. Tang, D. Sun, H. Wang, X. Huang, H. Zhang, S. Liu and Y. Liu, *RSC Adv.*, 2014, 4, 8328.
25. S. Liang, J. Zhou, G. Fang, X. Li, A. Pan, J. Wu, Y. Tang and J. Liu, *J. Alloys Comp.*, 2014, 583, 351-356.
26. H. He, G. Jin, H. Wang, X. Huang, Z. Chen, D. Sun and Y. Tang, *J. Mater. Chem. A*, 2014, 2, 3563.
27. H. Song, Y. Liu, C. Zhang, C. Liu and G. Cao, *J. Mater. Chem. A*, 2015, 3, 3547-3558.
28. S. Huang, X. L. Wang, Y. Lu, X. M. Jian, X. Y. Zhao, H. Tang, J. B. Cai, C. D. Gu and J. P. Tu, *J. Alloys Comp.*, 2014, 584, 41-46.
29. H. Wang, S. Liu, Y. Ren, W. Wang and A. Tang, *Energy Environ. Sci.*, 2012, 5, 6173.

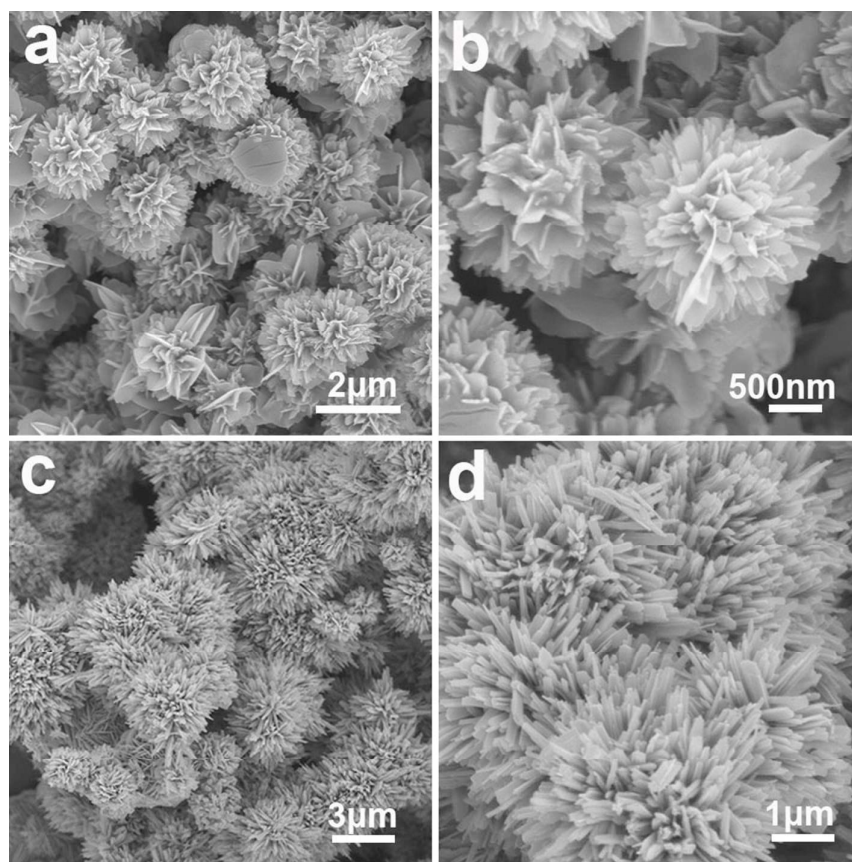
30. A. Q. Pan, H. B. Wu, L. Zhang and X. W. Lou, *Energy Environ. Sci.*, 2013, 6, 1476.
31. Y. L. Ding, Y. Wen, C. Wu, P. A. van Aken, J. Maier and Y. Yu, *Nano Lett.*, 2015, 15, 1388-1394.
32. S. H. Bae, S. Lee, H. Koo, L. Lin, B. H. Jo, C. Park and Z. L. Wang, *Adv. Mater.*, 2013, 25, 5098-5103.
33. S. Liang, J. Zhou, G. Fang, J. Liu, Y. Tang, X. Li and A. Pan, *ACS Appl. Mater. interfaces*, 2013, 5, 8704-8709.
34. C. Wang, Z. Guo, W. Shen, Q. Xu, H. Liu and Y. Wang, *Adv. Funct. Mater.*, 2014, 24, 5511-5521.
35. D. Sun, G. Jin, H. Wang, X. Huang, Y. Ren, J. Jiang, H. He and Y. Tang, *J. Mater. Chem. A*, 2014, 2, 8009.
36. L. Liang, Y. Xu, Y. Lei and H. Liu, *Nanoscale*, 2014, 6, 3536-3539.
37. C. Han, Y. Pi, Q. An, L. Mai, J. Xie, X. Xu, L. Xu, Y. Zhao, C. Niu, A. M. Khan and X. He, *Nano Lett.*, 2012, 12, 4668-4673.
38. R. Baddour-Hadjean, S. Bach, N. Emery and J. P. Pereira-Ramos, *J. Mater. Chem.*, 2011, 21, 11296.
39. S. Liang, J. Zhou, G. Fang, C. Zhang, J. Wu, Y. Tang and A. Pan, *Electrochim. Acta*, 2014, 130, 119-126.
40. G. Nagaraju, S. Sarkar, J. Dupont and S. Sampath, *Solid State Ionics*, 2012, 227, 30-38.
41. H. Liu, Y. Wang, L. Li, K. Wang, E. Hosono and H. Zhou, *J. Mater. Chem.*, 2009, 19, 7885.
42. Y. Xu, X. Han, L. Zheng, W. Yan and Y. Xie, *J. Mater. Chem.*, 2011, 21, 14466.
43. N. T. Hong Trang, N. Lingappan, I. Shakir and D. J. Kang, *J. Power Sources*, 2014, 251,

237-242.

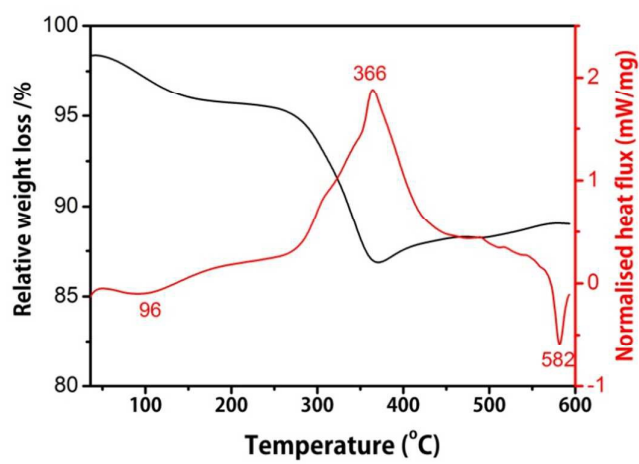
44. S. Liang, J. Zhou, X. Zhang, Y. Tang, G. Fang, T. Chen and X. Tan, *CrystEngComm*, 2013, 15, 9869.
45. H. Wang, K. Huang, C. Huang, S. Liu, Y. Ren and X. Huang, *J. Power Sources*, 2011, 196, 5645-5650.

**Figures and captions:**

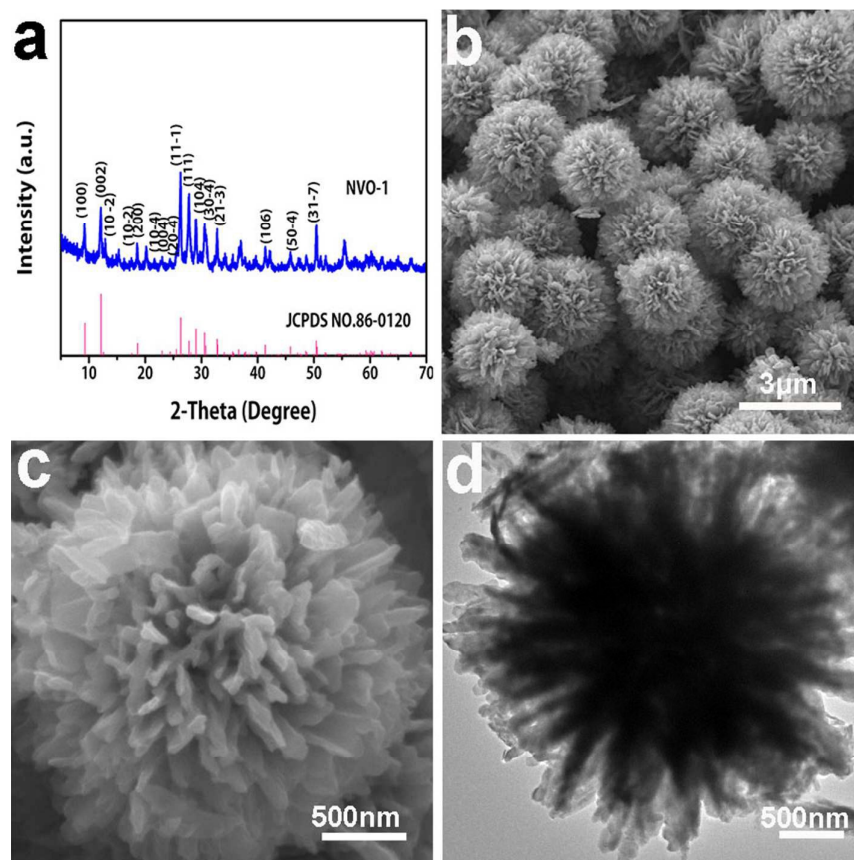
**Fig. 1** FESEM images of the hierarchical microspheres precursor solvothermally prepared at 180 °C for 48 hours (NVO-1 precursor).



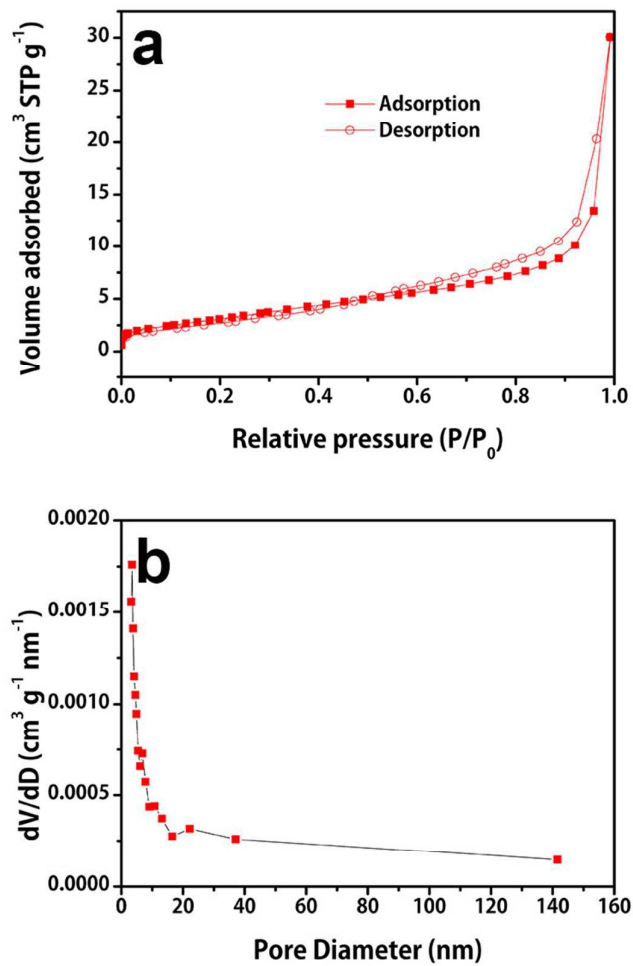
**Fig. 2** FESEM images of the hierarchical microflowers solvothermally prepared after changing the amount of  $\text{NaHCO}_3$ : (a and b), NVO-2 precursor; (c and d), NVO-3 precursor.



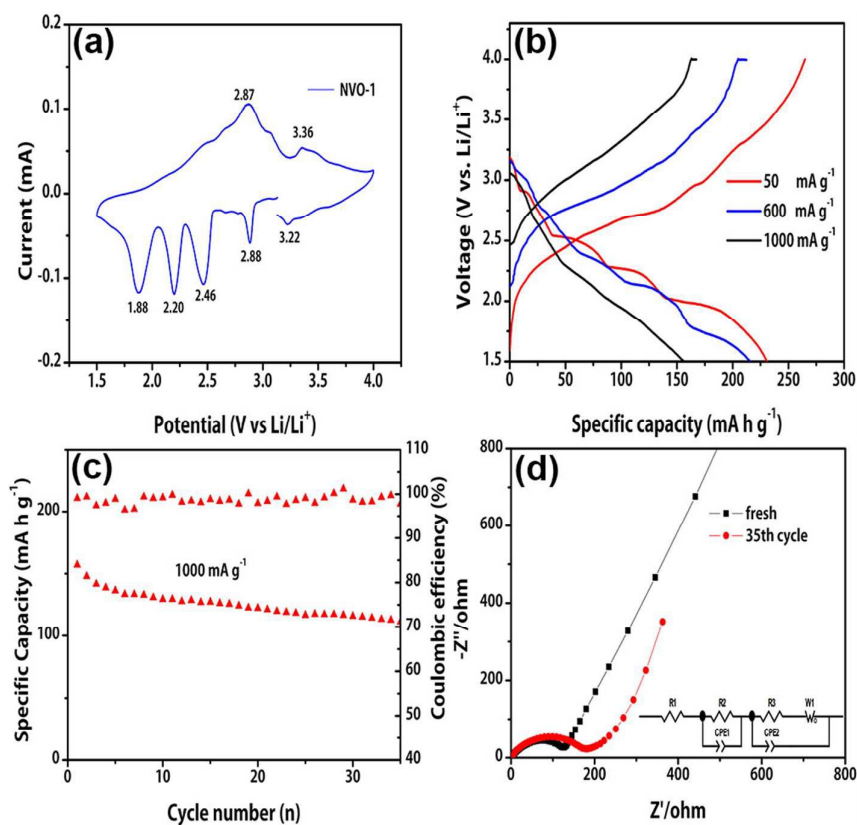
**Fig. 3** TG and DSC results for the as-obtained precursor after solvothermal process. The heating rate was set to  $10\text{ }^{\circ}\text{C min}^{-1}$ .



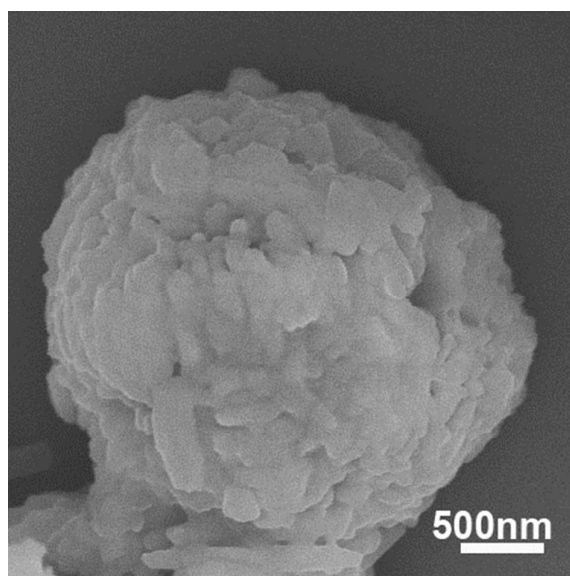
**Fig. 4** (a) XRD pattern, (b and c) FESEM images and (d) TEM image of the as-synthesized  $\beta$ - $\text{Na}_{0.33}\text{V}_2\text{O}_5$  microspheres (NVO-1) obtained by annealing the precursor microspheres at 400 °C for 3 h.



**Fig. 5** (a) Nitrogen adsorption-desorption isotherms and (b) the corresponding pore size distributions of the  $\beta$ -Na<sub>0.33</sub>V<sub>2</sub>O<sub>5</sub> microspheres

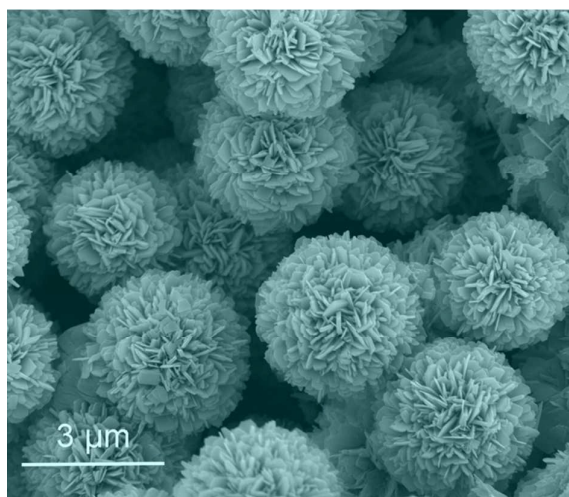


**Fig. 6** (a) Typical cyclic voltammograms (CV) curve of the  $\beta\text{-Na}_{0.33}\text{V}_2\text{O}_5$  microspheres at a scan rate of  $0.1 \text{ mV s}^{-1}$ ; (b) Discharge-charge profiles of the  $\beta\text{-Na}_{0.33}\text{V}_2\text{O}_5$  microspheres in the first two cycles at current densities of  $50$ ,  $600$  and  $1000 \text{ mA g}^{-1}$ ; (c) Cycling performance of the  $\beta\text{-Na}_{0.33}\text{V}_2\text{O}_5$  microspheres in the voltage range of  $1.5\text{-}4.0\text{V}$  at high current density of  $1000 \text{ mA g}^{-1}$ . (d) Nyquist plots of the  $\beta\text{-Na}_{0.33}\text{V}_2\text{O}_5$  microspheres electrodes at fresh state and after 35 cycles charged to  $4\text{V}$ .



**Fig. 7** Morphological analysis of the  $\beta\text{-Na}_{0.33}\text{V}_2\text{O}_5$  microspheres cycled for 35 cycles at current density of 1000  $\text{mA g}^{-1}$ .

## Graphic Abstract



Hierarchical nanosheet-assembled  $\beta\text{-Na}_{0.33}\text{V}_2\text{O}_5$  microspheres have been fabricated by a solvothermal method with subsequent calcinations in air, and exhibit high specific capacity and good rate capability.